

Fast exponential time integration for pricing options in stochastic volatility jump diffusion models

Hong-Kui Pang* Hai-Wei Sun†

Abstract

The stochastic volatility jump diffusion model with jumps both in return and volatility leads to a two dimensional partial integro-differential equation (PIDE). We exploit a fast exponential time integration scheme to solve this PIDE. After spatial discretization and temporal integration, the solution of the PIDE can be formulated as the action of an exponential of a block Toeplitz matrix on a vector. The shift-invert Arnoldi method is employed to approximate this product. To reduce the computational cost, the matrix splitting technique combined with the multigrid method is utilized to deal with the shift-invert matrix-vector product in each inner iteration. Numerical results show that the proposed scheme is more robust and efficient even compared with the existing high accurate implicit-explicit Euler based extrapolation scheme.

Key words: Stochastic volatility jump diffusion, European option, barrier option, partial integro-differential equation, matrix exponential, shift-invert Arnoldi, matrix splitting, multigrid method

Mathematics Subject Classification: 91B28, 62P05, 35K15, 65F10, 65M06, 91B70, 47B35

1 Introduction

In 1973, Black and Scholes [4] firstly developed a model to compute the price of a European option in the finance industry. Later empirical evidences indicate that the model assumptions on the log-normality of the return of the underlying asset and constant volatility are usually inconsistent with market prices [24, 29]. Several extensions of the Black-Scholes model have been proposed. Examples include the jump diffusion [19, 24] or pure jump

*School of Mathematics and Statistics, Jiangsu Normal University, Xuzhou, China. E-mail: panghongkui@163.com. This author was supported by the National Natural Science Foundation of China under grant 11201192, the Natural Science Foundation of Jiangsu Province under grant BK2012577, and the Natural Science Foundation for Colleges and Universities in Jiangsu Province under grant 12KJB110004.

†Department of Mathematics, University of Macau, Macao, China. E-mail: HSun@umac.mo. This author was supported by research grants 033/2009/A and 005/2012/A1 from FDCT and MYRG206(Y1-L4)-FST11-SHW from University of Macau.

Lévy models [2, 6, 7, 11, 23], stochastic volatility (SV) model [15, 18], stochastic volatility with jumps in return (SVJ) model [3], and stochastic volatility with correlated and contemporaneous jumps in return and variance (SVCJ) model [10, 13]. Among them, the SVCJ model usually offers much better match with market prices than others, since this model allows the volatility to be stochastic and can capture the jumps both in return and variance very well. In this paper, we consider the option valuation in the SVCJ model.

One of the way to price options is related to solving a partial integro-differential equation (PIDE). For the SVCJ model, the corresponding PIDE is a two dimensional equation which comprises a convolution integral defined over an infinite domain. D'Halluin et al. [9] propose a second-order accurate Crank-Nicolson scheme plus Rannacher time-stepping to approximate PIDEs. Nevertheless the direct application of the Crank-Nicolson scheme to the PIDE arising in the SVCJ model will suffer from the inversion of a block dense matrix at each time step. Andersen and Andreasen [1] use an operator splitting type of approach combined with a fast Fourier transform (FFT) evaluation of a convolution integral to price European options with jump diffusion. But this method can not easily handle the multidimensional jump diffusion processes and processes with state-dependent jump magnitude distributions as mentioned in [14]. Recently, an extrapolation scheme based on the implicit-explicit (IMEX) Euler method is proposed by Feng and Linetsky [14] to deal with the jump-diffusion PIDE. This method treats the differential term implicitly for stability and the integral term explicitly for numerical efficiency. Combined with the extrapolation approach, this method is remarkably fast and can achieve a polynomial accuracy in time direction. Zhang et al. [34] further improve the efficiency of the extrapolation scheme by coupling with the quadratic finite element for spatial discretization and preconditioning techniques for resulting systems. It is known that the IMEX Euler based extrapolation scheme belongs to the time-stepping method. When the time interval is large, many time steps may be required in order to achieve a given accuracy, which is very time consuming. Instead of using the time-stepping scheme, the authors in [28, 32] propose to exploit the exponential time integration (ETI) scheme to solve PIDEs arising from both the Black-Scholes and Merton's models. The advantage of the ETI scheme is that it is a one step method and hence we need not to discuss its stability and temporal discretized accuracy.

Our work here concerns the application of the ETI scheme for pricing options in the SVCJ model. Note that by the application of the ETI scheme, the price of an option involves the product of a matrix exponential and a vector. In [28, 32], the corresponding matrix exponential was directly computed by the scaling and squaring algorithm with Padé's approximation [16] which has an $\mathcal{O}(n^3)$ complexity, where n is the matrix size. While, what we finally need is the product of a matrix exponential and a vector but not the exact matrix exponential. For such case, the recent developed Krylov subspace methods [12, 17, 22, 25, 33] often work very well. Most recently, Lee, Liu, and Sun [20] employ the shift-invert Arnoldi method proposed in [21] to carry out the ETI scheme for pricing of options in Merton's [24] and Kou's [19] jump-diffusion models. By making use of the Toeplitz structure of the resulting matrix and the noted Gohberg-Semencul formula (GSF) for the inversion of the Toeplitz matrix, they reduce the computational cost of

the ETI scheme dramatically to $\mathcal{O}(n \log n)$ operations. Notice that for the PIDE arising in the SVCJ model, it has two space variables which are related to the asset price and the volatility respectively. After the spatial discretization of this PIDE by the central difference method and temporal integration of the semi-discretized ODE system by the ETI scheme, we obtain a solution vector formulated by the product of the exponential of a block Toeplitz matrix and a vector. When the shift-invert Arnoldi method is applied to approximate this solution vector, a shifted and inverted block Toeplitz matrix multiplied by a vector must be dealt with in each iteration step. Note that the resulting matrix here is block Toeplitz but not exact Toeplitz. Therefore no any efficient inversion formula, just like the GSF for the standard Toeplitz matrix, is available for the block Toeplitz matrix. Thus it is inevitable to lead to the inner-outer iteration. In order to relief the computational burden, a matrix splitting technique combined with a multigrid method is proposed to the inner iteration. Numerical results show that the proposed scheme is robust and efficient even compared with the high accurate IMEX Euler based extrapolation scheme.

The rest of this paper is arranged as follows. In Section 2, we recall the PIDE formulation for options valuation in the SVCJ model and perform the spatial discretization as well as the temporal integration. In Section 3, we introduce the shift-invert Arnoldi method and present an algorithm for fast implementation of ETI scheme. Numerical comparisons between the ETI scheme and the IMEX Euler based extrapolation scheme are shown in Section 4. At last, concluding remarks are given in Section 5.

2 Discretization of the PIDE in the SVCJ model

We firstly recall the PIDE arising in the SVCJ model. For more details of the equation, we refer readers to [13, 14, 34]. Let $u(t, x, y)$ denote the option price of a European-style option if at time $\bar{T} - t$ the underlying asset price equals Ke^x and its instantaneous variance equals $(1 + y)\theta$, where \bar{T} refers to the maturity time, K is the strike price, and θ stands for the long-run variance level. According to [14, 34], the option value function $u(t, x, y)$ in the SVCJ model satisfies the following two-dimensional PIDE:

$$u_t = \mathcal{A}u + \mathcal{B}u, \quad t \in (0, \bar{T}], \quad (x, y) \in \Omega, \quad (2.1)$$

where

$$\begin{aligned} \mathcal{A}u &= \frac{1}{2}\theta(y+1)u_{xx} + \rho_D\zeta(y+1)u_{xy} + \frac{\zeta^2}{2\theta}(y+1)u_{yy} \\ &\quad + \left[\mu - \frac{1}{2}\theta(y+1) \right] u_x - \kappa y u_y - (r + \lambda)u, \\ \mathcal{B}u &= \lambda \int_{-\infty}^{\infty} \int_0^{\infty} u(t, x + z^x, y + z^y) p(z^x, z^y) dz^y dz^x \end{aligned}$$

with the joint probability density

$$p(z^x, z^y) = \frac{\theta}{\nu\sqrt{2\pi\sigma_J^2}} \exp \left[-\frac{\theta z^y}{\nu} - \frac{(z^x - \mu_J - \rho_J\theta z^y)^2}{2\sigma_J^2} \right], \quad z^x \in \mathbb{R}, \quad z^y \geq 0. \quad (2.2)$$

Here the parameter ρ_D is the correlation coefficient correlating Brownian shocks in the return and variance processes, ζ is the volatility-of-volatility parameter,

$$\mu = r - q + \lambda[1 - (1 - \nu\rho_J)^{-1} \exp(\mu_J + \sigma_J^2/2)]$$

is the drift parameter, κ is the rate of mean reversion, r is the risk-free interest rate, q is the dividend rate, λ is the intensity of compound Poisson process, and $\nu, \mu_J, \rho_J, \sigma_J$ are parameters related to jumps in return and variance.

As stated in [14, 34], the spatial domain Ω in (2.1) depends on the option that we investigate. In this paper, two types of options are considered, the European vanilla option and the double barrier option. Theoretically, the domain $\Omega = (-\infty, +\infty) \times (-1, +\infty)$ for the vanilla option and $\Omega = (x_L, x_R) \times (-1, +\infty)$ for the double barrier option with lower barrier L and upper barrier U , where $x_L = \ln(L/K)$ and $x_R = \ln(U/K)$. To render the numerical solution feasible: the spatial domain is restricted to a bounded set $(x_{\min}, x_{\max}) \times (y_{\min}, y_{\max})$ with $y_{\min} = -1$ and fixed x_{\min}, x_{\max} , and y_{\max} chosen sufficiently large. Specially, for the double barrier option, $x_{\min} = x_L$ and $x_{\max} = x_R$. For convenience, the bounded set $(x_{\min}, x_{\max}) \times (y_{\min}, y_{\max})$ is still denoted by Ω .

The initial condition for (2.1) is given by

$$u(0, x, y) = \psi(x, y), \quad (x, y) \in \Omega$$

with $\psi(x, y)$ being the payoff function. For a European call option $\psi(x, y) = K(e^x - 1)^+$, whereas for a put option $\psi(x, y) = K(1 - e^x)^+$, where $x^+ = \max\{x, 0\}$.

Next, Dirichlet boundary conditions are imposed on the complement of the bounded set $\Omega = (x_{\min}, x_{\max}) \times (y_{\min}, y_{\max})$ [14, 34]:

$$u(t, x, y) = \phi(x, y), \quad (x, y) \in \Omega^c,$$

where Ω^c represents the complement of Ω in the whole plane. In general, $\phi = \psi$ for the European vanilla option and $\phi = 0$ for the double barrier option; see [14, 34] for more discussions.

In the following, we show how to discretize the PIDE (2.1) and transform it into a matrix exponential problem.

2.1 Spatial discretization

Let the spatial domain of (2.1) be restricted to $\Omega = (x_{\min}, x_{\max}) \times (y_{\min}, y_{\max})$ and define a computational grid $\Omega_{h_x, h_y} = \{(x_i, y_j), 0 \leq i \leq m, 0 \leq j \leq n\}$ with

$$\begin{cases} x_i = x_{\min} + ih_x, & h_x = \frac{x_{\max} - x_{\min}}{m}, & i = 0, 1, \dots, m, \\ y_j = y_{\min} + jh_y, & h_y = \frac{y_{\max} - y_{\min}}{n}, & j = 0, 1, \dots, n. \end{cases}$$

We approximate the differential term $\mathcal{A}u$ in (2.1) by the second-order central difference scheme. Let $u_{i,j}(t)$ denote the approximation to $u(t, x_i, y_j)$ and $\mathbf{u}(t) = [\mathbf{u}_1(t), \dots, \mathbf{u}_{m-1}(t)]^\top$

with $\mathbf{u}_i(t) = [u_{i,1}(t), \dots, u_{i,n-1}(t)]$ for $i = 1, \dots, m-1$. Then the differential term $\mathcal{A}u$ has the discretization form

$$\mathbf{A}u(t) + \mathbf{f}_A,$$

where A is a block tri-diagonal Toeplitz matrix

$$A = \begin{bmatrix} A_{(0)} & A_{(1)} & & 0 \\ A_{(-1)} & A_{(0)} & \ddots & \\ & \ddots & \ddots & A_{(1)} \\ 0 & & A_{(-1)} & A_{(0)} \end{bmatrix} \in \mathbb{R}^{(m-1)(n-1) \times (m-1)(n-1)} \quad (2.3)$$

with tri-diagonal blocks $A_{(-1)}, A_{(0)}, A_{(1)} \in \mathbb{R}^{(n-1) \times (n-1)}$, which are given respectively by

$$\begin{aligned} A_{(-1)} &= D_{n-1} \cdot \text{tridiag} \left(\frac{\rho D \zeta}{4h_x h_y}, \frac{\theta}{2h_x^2} + \frac{\theta}{4h_x}, -\frac{\rho D \zeta}{4h_x h_y} \right) - \frac{\mu}{2h_x} I, \\ A_{(0)} &= D_{n-1} \cdot \text{tridiag} \left(\frac{\zeta^2}{2\theta h_y^2} + \frac{\kappa}{2h_y}, -\frac{\theta}{h_x^2} - \frac{\zeta^2}{\theta h_y^2}, \frac{\zeta^2}{2\theta h_y^2} - \frac{\kappa}{2h_y} \right) \\ &\quad + \text{tridiag} \left(-\frac{\kappa}{2h_y}, -(r + \lambda), \frac{\kappa}{2h_y} \right), \\ A_{(1)} &= D_{n-1} \cdot \text{tridiag} \left(-\frac{\rho D \zeta}{4h_x h_y}, \frac{\theta}{2h_x^2} - \frac{\theta}{4h_x}, \frac{\rho D \zeta}{4h_x h_y} \right) + \frac{\mu}{2h_x} I, \end{aligned}$$

$D_{n-1} = \text{diag}(y_1 + 1, \dots, y_{n-1} + 1)$, I is the identity matrix, the vector \mathbf{f}_A is the load vector. Note that for the double barrier option, \mathbf{f}_A is equal to zero due to the zero boundary condition.

For the integral term $\mathcal{B}u$, at each inner grid point (x_i, y_j) , $i = 1, \dots, m-1$ and $j = 1, \dots, n-1$, we first change variables and then split the integral into two parts

$$\begin{aligned} \mathcal{B}u(t, x_i, y_j) &= \lambda \int_{-\infty}^{\infty} \int_0^{\infty} u(t, x_i + z^x, y_j + z^y) p(z^x, z^y) dz^y dz^x \\ &= \lambda \int_{-\infty}^{\infty} \int_{y_j}^{\infty} u(t, \omega, \eta) p(\omega - x_i, \eta - y_j) d\eta d\omega \\ &= \lambda \int_{x_{\min}}^{x_{\max}} \int_{y_j}^{y_{\max}} u(t, \omega, \eta) p(\omega - x_i, \eta - y_j) d\eta d\omega \\ &\quad + \lambda \iint_{\Omega_j^*} u(t, \omega, \eta) p(\omega - x_i, \eta - y_j) d\eta d\omega, \end{aligned} \quad (2.4)$$

where $\Omega_j^* = (-\infty, \infty) \times (y_j, \infty) \setminus (x_{\min}, x_{\max}) \times (y_j, y_{\max})$. For the first part of (2.4), we use the composite trapezoidal rule with step sizes h_x and h_y in x and y directions respectively

and obtain the approximation

$$\begin{aligned} & \lambda \int_{x_{\min}}^{x_{\max}} \int_{y_j}^{y_{\max}} u(t, \omega, \eta) p(\omega - x_i, \eta - y_j) d\eta d\omega \\ & \approx \lambda \frac{h_x h_y}{4} (p_{-i,0} u_{0,j} + p_{m-i,0} u_{m,j} + p_{-i,n-j} u_{0,n} + p_{m-i,n-j} u_{m,n} + 2 \sum_{k=1}^{m-1} p_{k-i,0} u_{k,j} \\ & \quad + 2 \sum_{k=1}^{m-1} p_{k-i,n-j} u_{k,n} + 2 \sum_{l=j+1}^{n-1} p_{-i,l-j} u_{0,l} + 2 \sum_{l=j+1}^{n-1} p_{m-i,l-j} u_{m,l} + 4 \sum_{k=1}^{m-1} \sum_{l=j+1}^{n-1} p_{k-i,l-j} u_{k,l}), \end{aligned}$$

where $p_{k-i,l-j} = p(x_k - x_i, y_l - y_j)$ for $k = 0, 1, \dots, m$ and $l = 0, 1, \dots, n$. Rewriting all these approximations into the matrix form yields the following vector

$$B\mathbf{u}(t) + \mathbf{f}_{B_1},$$

where the matrix B is a block Toeplitz matrix with Toeplitz blocks (BTTB) given by

$$B = \begin{bmatrix} B_{(0)} & B_{(1)} & \cdots & B_{(m-2)} \\ B_{(-1)} & B_{(0)} & \ddots & \vdots \\ \vdots & \ddots & \ddots & B_{(1)} \\ B_{(-(m-2))} & \cdots & B_{(-1)} & B_{(0)} \end{bmatrix} \in \mathbb{R}^{(m-1)(n-1) \times (m-1)(n-1)}, \quad (2.5)$$

each block $B_{(k)}$ has the form

$$B_{(k)} = \begin{bmatrix} b_0^k & b_1^k & \cdots & b_{n-2}^k \\ 0 & b_0^k & \ddots & \vdots \\ \vdots & \ddots & \ddots & b_1^k \\ 0 & \cdots & 0 & b_0^k \end{bmatrix} \in \mathbb{R}^{(n-1) \times (n-1)}$$

with $b_0^k = \frac{1}{2} \lambda h_x h_y p_{k,0}$ and $b_l^k = \lambda h_x h_y p_{k,l}$, $k = 0, \pm 1, \dots, \pm(m-2)$, $l = 1, \dots, n-2$, the vector \mathbf{f}_{B_1} is the load vector. Again for the double barrier option, the vector \mathbf{f}_{B_1} is equal to zero for the zero boundary condition.

The value of the second part in (2.4) completely depends on the option contract to be priced. If the option of interest is the double barrier option, then the value is naturally equal to zero because of the zero boundary condition $\phi = 0$. If the option of concern is the vanilla put option, then the option price $u(t, x, y)$ over Ω_* is given by $\phi(x, y) = K(1 - e^x)^+$, and thus

$$\begin{aligned} & \lambda \iint_{\Omega_j^*} u(t, \omega, \eta) p(\omega - x_i, \eta - y_j) d\eta d\omega \\ & = \lambda \int_{-\infty}^{x_{\min}} \int_{y_j}^{\infty} K(1 - e^\omega) p(\omega - x_i, \eta - y_j) d\eta d\omega \\ & \quad + \lambda \int_{x_{\min}}^0 \int_{y_{\max}}^{\infty} K(1 - e^\omega) p(\omega - x_i, \eta - y_j) d\eta d\omega. \end{aligned} \quad (2.6)$$

Substituting the probability density function (2.2) into (2.6) and by some calculations, we obtain

$$\begin{aligned} & \lambda \int_{-\infty}^{x_{\min}} \int_{y_j}^{\infty} K(1 - e^{\omega}) p(\omega - x_i, \eta - y_j) d\eta d\omega \\ &= \frac{\lambda K \theta}{\nu} \left(\int_0^{\infty} e^{-\frac{\theta \xi}{\nu}} \mathcal{N}(\chi_i(\xi)) d\xi - e^{x_i + \frac{\sigma_J^2}{2} + \mu_J} \int_0^{\infty} e^{(\rho_J - \frac{1}{\nu})\theta \xi} \mathcal{N}(\chi_i(\xi) - \sigma_J) d\xi \right) \end{aligned}$$

and

$$\begin{aligned} & \lambda \int_{x_{\min}}^0 \int_{y_{\max}}^{\infty} K(1 - e^{\omega}) p(\omega - x_i, \eta - y_j) d\eta d\omega \\ &= \frac{\lambda K \theta}{\nu} \left(\int_{y_{\max} - y_j}^{\infty} e^{-\frac{\theta \xi}{\nu}} \left(\mathcal{N}\left(\chi_i(\xi) - \frac{x_{\min}}{\sigma_J}\right) - \mathcal{N}(\chi_i(\xi)) \right) d\xi \right. \\ & \quad \left. - e^{x_i + \frac{\sigma_J^2}{2} + \mu_J} \int_{y_{\max} - y_j}^{\infty} e^{(\rho_J - \frac{1}{\nu})\theta \xi} \left(\mathcal{N}\left(\chi_i(\xi) - \frac{x_{\min} + \sigma_J^2}{\sigma_J}\right) - \mathcal{N}(\chi_i(\xi) - \sigma_J) \right) d\xi \right), \end{aligned}$$

where $\mathcal{N}(\cdot)$ is the standard normal cumulative distribution function and

$$\chi_i(\xi) = \frac{x_{\min} - x_i - \mu_J - \rho_J \theta \xi}{\sigma_J}, \quad i = 1, 2, \dots, m-1.$$

Since the integrands in above integrals decay rapidly as the variable of integration ξ approaches to infinity, we can evaluate these integrals efficiently using numerical integration methods, such as the adaptive Gauss-Kronrod quadrature method [31]. The obtained value of (2.6) is taken as the $((i-1)(n-1) + j)$ -th element of a vector \mathbf{f}_{B_2} . We note that for the vanilla call option, the second part in (2.4) can also be computed similarly as above.

After collecting all these discretization terms together, we obtain the semi-discretized form of (2.1), which is an ODE system

$$\frac{d\mathbf{u}(t)}{dt} = A\mathbf{u}(t) + B\mathbf{u}(t) + \mathbf{f}, \quad t \in (0, \bar{T}], \quad (2.7)$$

where A and B are given by (2.3) and (2.5) respectively, and $\mathbf{f} = \mathbf{f}_A + \mathbf{f}_{B_1} + \mathbf{f}_{B_2}$.

2.2 Temporal integration

Rather than employing the time-stepping method for (2.7), in this paper we consider the ETI scheme which has been used in [20, 28, 32] for option pricing problems in one dimensional models. After integrating (2.7) over the time interval $(0, \bar{T}]$, we obtain the solution

$$\mathbf{u}(\bar{T}) = e^{\bar{T}(A+B)} \mathbf{u}(0) + \int_0^{\bar{T}} e^{(\bar{T}-t)(A+B)} \mathbf{f} dt$$

at the maturity time \bar{T} , where $\mathbf{u}(0)$ is the initial vector containing the discrete values of the payoff function $\psi(x, y)$. From the assumptions on boundary conditions we see that

the vector \mathbf{f} is independent of the time t . Therefore the solution can be explicitly written as

$$\mathbf{u}(\bar{T}) = e^{\bar{T}(A+B)}(\mathbf{u}(0) + (A+B)^{-1}\mathbf{f}) - (A+B)^{-1}\mathbf{f}. \quad (2.8)$$

Different from the time-stepping method, the ETI scheme is an exact method and does not require the discretization in time direction.

In terms of (2.8), to evaluate the option price $\mathbf{u}(\bar{T})$ at the maturity time \bar{T} , one has to compute the term $(A+B)^{-1}\mathbf{f}$ and the product of the matrix exponential $e^{\bar{T}(A+B)}$ and a vector. By (2.3) and (2.5), we know that both matrices A and B in (2.8) are block Toeplitz matrices, so is the matrix $A+B$. Thus the term $(A+B)^{-1}\mathbf{f}$ can be computed using preconditioned Krylov subspace methods with block circulant preconditioners [8] or other fast solvers, such as the multigrid method [5]. Moreover, for the double barrier option, this term is vanished, i.e., $\mathbf{f} = 0$. Hence, the main workload in (2.8) is to compute the product of a block Toeplitz matrix exponential and a vector. As mentioned in Section 1, the direct computation of the matrix exponential is prohibited because of its cubic operation cost with respect to the matrix size [16]. To improve the performance of the ETI scheme, we adopt the shift-invert Arnoldi method coupled with the multigrid solver to fast approximate the product $e^{\bar{T}(A+B)}v$ for some vector v .

3 Shift-invert Arnoldi method

3.1 Shift-invert Arnoldi method

Over the past two decades, the Krylov subspace methods as a class of efficient methods to deal with the product of a large matrix exponential and a vector have been investigated intensively [12, 17, 22, 25, 33]. The standard approach to approximate the product $e^{T_n}v$ with $T_n \in \mathbb{R}^{n \times n}$ and $v \in \mathbb{R}^n$ is to first establish an orthonormal base $V_m = [v_1, v_2, \dots, v_m]$ of the Krylov subspace $\mathcal{K}_m(T_n, v) = \text{span}\{v, T_nv, \dots, T_n^{m-1}v\}$. This can be done using the Arnoldi process for the nonsymmetric matrix or the Lanczos process for the symmetric matrix. The result is summarized in the following matrix formulation:

$$T_n V_m = V_m H_m + h_{m+1,m} v_{m+1} e_m^*,$$

where H_m is the m -by- m projected matrix, e_m is the m -th canonical basis vector, and v_{m+1} is a unit vector that satisfies $V_m^* v_{m+1} = 0$. Then the vector $e^{T_n}v$ is approximated by [30]

$$e^{T_n}v \approx \beta V_m e^{H_m} e_1, \quad \beta = \|v\|_2,$$

with $\|\cdot\|_2$ being the spectral norm. It is clearly that the Krylov subspace method reduces the problem of approximating the vector $e^{T_n}v$ where T_n is a large n -by- n matrix to that of computing the vector $e^{H_m}e_1$ where H_m is a smaller m -by- m matrix. Moreover, only the matrix-vector product is needed during the whole process. When the Krylov subspace method is carried out, it naturally hopes that the iteration number m is as small as possible in order to achieve a given accuracy. However, theoretical analyses [17, 30] show that the

error decay is generally related to the norm $\|T_n\|_2$ and therefore the iterative number m could get quite large as $\|T_n\|_2$ increases,

To accelerate the approximation process of the Krylov subspace method, the authors in [25, 33] propose to use the shift-invert preconditioning technique. The motivation comes from the observation that the exponential function is a quickly decaying function and the vector $e^{T_n}v$ is mostly determined by small module eigenvalues and their corresponding invariant subspaces provided that the spectrum of T_n is contained in the left half plane. The concrete practice of this preconditioning technique is as follows. Firstly, the product $e^{T_n}v$ is rewritten in

$$e^{T_n}v = e^{-\frac{1}{\gamma}((I-\gamma T_n)^{-1})^{-1}-I}v,$$

where I is the identity matrix and $\gamma > 0$ is a shift parameter. Then we construct an orthonormal base $\widehat{V}_m = [\widehat{v}_1, \widehat{v}_2, \dots, \widehat{v}_m]$ of the Krylov subspace $\mathcal{K}_m((I - \gamma T_n)^{-1}, v)$ using the Arnoldi (or Lanczos) process, which leads to the following relations

$$(I - \gamma T_n)^{-1}\widehat{V}_m = \widehat{V}_m\widehat{H}_m + \widehat{h}_{m+1,m}\widehat{v}_{m+1}e_m^*, \quad \widehat{V}_m^*\widehat{v}_{m+1} = 0.$$

Finally, the vector $e^{-\frac{1}{\gamma}((I-\gamma T_n)^{-1})^{-1}-I}v$ is approximated by

$$e^{-\frac{1}{\gamma}((I-\gamma T_n)^{-1})^{-1}-I}v \approx \beta\widehat{V}_me^{-\frac{1}{\gamma}(\widehat{H}_m^{-1}-I)}e_1, \quad \beta = \|v\|_2. \quad (3.1)$$

The whole process is summarized in the following algorithm.

ALGORITHM 3.1: SHIFT-INVERT ARNOLDI METHOD FOR $e^{T_n}v$

-
1. Initialize: Compute $\beta = \|v\|_2$ and $\widehat{v}_1 = v/\beta$
 2. Iterate: Do $j = 1, \dots, m$
 - (a) Compute $w := (I - \gamma T_n)^{-1}\widehat{v}_j$
 - (b) Do $k = 1, \dots, j$
 - i. Compute $\widehat{h}_{k,j} := (w, \widehat{v}_k)$
 - ii. Compute $w := w - \widehat{h}_{k,j}\widehat{v}_k$
 - (c) Compute $\widehat{h}_{j+1,j} := \|w\|_2$ and $\widehat{v}_{j+1} := w/\widehat{h}_{j+1,j}$
 3. Approximation: $e^{T_n}v \approx \beta\widehat{V}_me^{-\frac{1}{\gamma}(\widehat{H}_m^{-1}-I)}e_1$
-

Both theoretical analyses and numerical experiments in [25, 33] show that this shift-invert preconditioning technique can speed up the approximation process dramatically provided that the matrix T_n is a sectorial operator. However, it is not easy to theoretically prove that the semidiscrete matrix $A + B$ is a sectorial operator. In Figure 1, we plot the eigenvalues of $A + B$ with the grid numbers $m = 16$ and $n = 128$ for the European vanilla put option. Model parameters are taken from Table 1. We can see from Figure 1 that all the eigenvalues are located in the left half plane. Numerical experiments in Section 4 also show the efficiency of the shift-invert Arnoldi method for our problems.

According to Algorithm 3.1, we have to compute the product $(I - \gamma T_n)^{-1}\widehat{v}_j$ in each iteration step. If T_n is a Toeplitz matrix, then this product can be computed very fast by the celebrated Toeplitz inverse formula GSF [20, 21, 26] by FFTs. However, for our

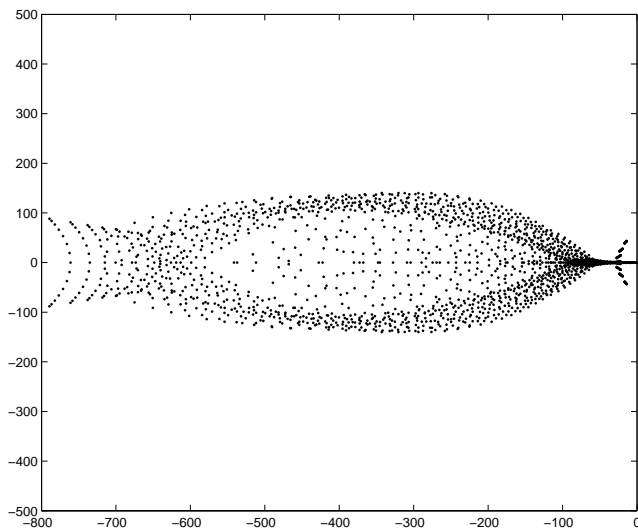


Figure 1: Eigenvalues of matrix $A + B$ with $m = 16$ and $n = 128$.

case, the matrix T_n is the sum of block Toeplitz matrices A and B , but not the exact Toeplitz matrix. Therefore the GSF can not be used anymore and we have to solve the linear system

$$(I - \gamma(A + B))w = \hat{v}_j \quad (3.2)$$

in each iteration step. In the following subsection, we propose to employ the matrix splitting technique combined with a multigrid method to fast solve this system.

3.2 Matrix splitting technique with multigrid method

Recall that the matrix A in (3.2) is a block tri-diagonal Toeplitz matrix with tri-diagonal blocks and B is a BTTB dense matrix. To avoid the inversion of a large dense matrix, we put B in the right hand side of (3.2) and build up the following iteration scheme:

$$(I - \gamma A)w_{k+1} = \gamma Bw_k + \hat{v}_j, \quad k = 0, 1, \dots, \quad (3.3)$$

where w_0 is an initial guess. Next, we exploit the multigrid method to solve these systems.

The multigrid method is one of the most efficient algorithms for linear systems arising from PDEs. The basic idea of multigrid is to employ relaxations on fine-grid to damp oscillatory errors and approximations on coarse-grid to smooth errors. For a general linear system

$$A_N w = b \quad (3.4)$$

with $A_N \in \mathbb{C}^{N \times N}$ and $b \in \mathbb{C}^N$, the commonly used procedure of the multigrid method is the V-cycle. Suppose we have provided a sequence of coarse grid operators A_{N_s} with $1 \leq s \leq l$, the relaxation operators $G_{N_s}: \mathbb{C}^{N_s} \rightarrow \mathbb{C}^{N_s}$ with ν_1 and ν_2 being the numbers of

pre- and post-relaxation steps respectively, the restriction operators $I_s^{s+1} : \mathbb{C}^{N_s} \rightarrow \mathbb{C}^{N_{s+1}}$, the interpolation operators $I_{s+1}^s : \mathbb{C}^{N_{s+1}} \rightarrow \mathbb{C}^{N_s}$ as well as the coarsest grid number N_l . Here l is the total number of grid levels, with $s = 1$ being the finest level. That is to say for $s = 1$, $A_{N_1} = A_N$. Then the V-cycle multigrid can be described as the algorithm below [5].

ALGORITHM 3.2: V-CYCLE

```

Procedure  MG( $\nu_1, \nu_2$ ) ( $w_s, b_s$ )
  If  $s = l$ 
     $w_l := A_{N_l}^{-1} b_l$ ;
  else
    for  $j = 1 : \nu_1$ 
       $w_s := G_{N_s} w_s + (I - G_{N_s}) A_{N_s}^{-1} b_s$ ;
    end
     $d_{s+1} := I_s^{s+1} (b_s - A_{N_s} w_s)$ ;
     $e_{s+1}^0 := 0$ ;
     $e_{s+1} := \text{MG}(\nu_1, \nu_2) (e_{s+1}^0, d_{s+1})$ ;
     $w_s := w_s + I_{s+1}^s e_{s+1}$ ;
    for  $j = 1 : \nu_2$ 
       $w_s := G_{N_s} w_s + (I - G_{N_s}) A_{N_s}^{-1} b_s$ ;
    end
  end
  MG( $\nu_1, \nu_2$ ) :=  $w_s$ ;
end

```

When Algorithm 3.2 is applied to solve the k -th system of (3.3), the finest grid operator, the unknown vector, and the right-hand side in (3.4) become

$$A_N = I - \gamma A, \quad w = w_{k+1}, \quad \text{and} \quad b = \gamma B w_k + \hat{v}_j,$$

where $N = (m - 1)(n - 1)$. We perform the V-cycle with full coarsening and set the total grid level $l = \log_2(\min\{m, n\})$. Then the coarse grid numbers $N_s = (\frac{m}{2^{s-1}} - 1)(\frac{n}{2^{s-1}} - 1)$ for $1 \leq s \leq l$. Note that the matrix A is a block tri-diagonal Toeplitz matrix with tri-diagonal blocks, so is A_N , which inspired us to use the block Gauss-Seidel relaxation operator [5]. In addition, we adopt the red-black strategy which does not add any computational cost. To retain the block tri-diagonal Toeplitz structure in coarse grid operators, we construct A_{N_s} by discretizing the PIDE (2.1) with coarse grid numbers. In other words, we define the coarse grid operators in geometric means. The restriction operators are defined as [5]

$$I_s^{s+1} = P \otimes P$$

4 Numerical experiments

In this section, we demonstrate numerically the efficiency of the proposed ETI scheme by comparing with the IMEX Euler based extrapolation scheme introduced in [14]. All experiments are performed in MATLAB 7.11 (R2010b) on a PC with configuration: Intel(R)Xeon(R)CPU W3520 @ 2.67GHz and 6.00GB RAM.

We consider the European vanilla put (EVP) option and the knock-out double barrier put (DBP) option under the SVCJ model. The corresponding payoff function is $\psi(x, y) = K(1 - e^x)^+$. Parameter values used in our numerical experiments are taken from [14, 34] and given in Table 1. Among them, λ , ν , μ_J , σ_J , ρ_D , ρ_J , ζ , κ , θ , r , q are model parameters and K is the strike price. Parameters L and U are the lower and upper barriers of the DBP option, respectively. In practical computations, the infinite domains of EVP and DBP options are restricted to bounded domains Ω_{EVP} and Ω_{DBP} , respectively. We call these bounded domains to be the computational domain. Numerical tests show that the computational domains given in Table 1 lead to small enough truncation errors for considered option prices.

Table 1: Parameter values used in numerical experiments.

Model and option parameters	$\lambda = 4$, $\nu = 0.02$, $\mu_J = -0.04$, $\sigma_J = 0.06$, $\rho_D = -0.5$, $\rho_J = -0.5$ $\zeta = 0.1$, $\kappa = 4$, $\theta = 0.04$, $r = 5\%$, $q = 2\%$, $K = 100$, $L = 80$, $U = 120$
Other parameters	$\Omega_{DBP} = (x_{\min}, x_{\max}) \times (y_{\min}, y_{\max}) = (\ln 0.8, \ln 1.2) \times (-1, 7)$, $\Omega_{EVP} = (x_{\min}, x_{\max}) \times (y_{\min}, y_{\max}) = (-0.8, 0.8) \times (-1, 7)$.

The ETI scheme is implemented by the the shift-invert Arnoldi method. In all tests, the shift parameter is chosen as $\gamma = 1/15$, the stop criterion adopts the formula (3.19) in [27], and the related tolerance is set to be 10^{-5} . In the inner iteration of the shift-invert Arnoldi process, we employ the matrix splitting iteration with multigrid method as described in Section 3.2 to solve the system (3.2). Only one V-cycle is carried out to the each step of the iteration scheme (3.3). In addition, the numbers of pre-correction relaxation sweep and post-correction relaxation sweep in the V-cycle are both set to be 1. As comparisons, we also use the same V-cycle to solve the resulting systems arising from the IMEX Euler based extrapolation scheme [14]. The extrapolation process is stopped when the local error tolerance is less than 10^{-5} . In both schemes, we stop solving the resulting systems when the relative residual error is less than 10^{-8} .

We first price a 3 month ($\bar{T} = 0.25$) EVP option which can also be obtained by inverting the Fourier transform by the FFT [10]. We investigate the pricing error at the at-the-money option with the asset price $S_0 = K = 100$ and the volatility $\sigma_0 = 20\%$, which corresponds to the point $(x, y) = (0, 0)$, since the asset price S , the volatility σ , x , and y have the relationships: $S = Ke^x$, $\sigma = \sqrt{\theta(y+1)}$. The benchmark price is computed using the FFT and is equal to 4.812582536. Table 2 reports the numerical results of the ETI scheme and the extrapolation scheme with different grid numbers. In

the table, the symbol “ (m,n) ” represents the number of spatial grid points, “ETI” and “Extrapolation” refer to the ETI scheme and the extrapolation scheme respectively, and “outer/inner” stands for the out iteration number and the average inner iteration number. We remark that for the ETI scheme, the outer iteration number refers to iteration steps of the Arnoldi process, and the inner iteration number refers to the average iteration number of the iteration scheme (3.3). For the extrapolation scheme, the outer iteration number refers to the number of resulting systems required to be solved in the extrapolation process, and the inner iteration number refers to the average iteration number of solving those systems. “CPUtime” denotes the total CPU time of performing the corresponding schemes with the unit in second. The label “Error” in the table represents the pricing error at the at-the-many option (i.e., at the point $(x, y) = (0, 0)$). The column “ratio” is the ratio of two consecutive pricing error.

Table 2: Numerical results for pricing the EVP option with maturity time $\bar{T} = 0.25$ by the ETI scheme and the extrapolation scheme respectively.

(m,n)	ETI		Extrapolation		Error	ratio
	out/inner	CPUtime	out/inner	CPUtime		
(16, 128)	11/6.09	0.15	45/5.22	0.37	4.20e-001	4.45
(32, 256)	14/6.00	0.46	45/7.11	1.38	9.44e-002	4.13
(64, 512)	14/6.07	1.65	45/7.89	4.49	2.29e-002	4.01
(128,1024)	16/7.00	8.47	45/8.00	16.31	5.70e-003	4.03
(256,2048)	18/7.06	41.22	45/8.00	68.75	1.41e-003	

Numerical results in columns “Error” and “ratio” show that numerical solutions converge to the benchmark and the convergence rate is the second order accuracy, which exemplify the correction of our proposed scheme. From Table 2, we see that to reach the same accuracy, the outer iteration number and the CPU time required by the ETI scheme are much less than that by the extrapolation scheme. In addition, the average inner iteration numbers for the ETI scheme are not large and almost independent of spatial grid numbers, which implies that the splitting iteration scheme (3.3) converges very fast and in each iteration step, one V-cycle is enough to approximate the solution of the iterative system.

To further illustrate the efficiency of the ETI scheme on other numerical aspects, we also price 3 month ($\bar{T} = 0.25$), 6 month ($\bar{T} = 0.5$), and 1 year ($\bar{T} = 1.0$) DBP options respectively. The pricing errors are investigated in the approximation domain $G = (\underline{x}_G, \bar{x}_G) \times (\underline{y}_G, \bar{y}_G) = (\ln 0.8, \ln 1.2) \times (0, 3)$ (corresponding to (80, 120) in the underlying asset price and (20%, 40%) in the volatility), where we are interested in the value function u . We compute the benchmark price with large enough grid numbers ($m = 320$ and $n = 2048$) using the ETI scheme. Tables 3, 4, and 5 display the numerical results for pricing DBP options with maturity times $\bar{T} = 0.25$, $\bar{T} = 0.5$, and $\bar{T} = 1.0$ respectively. In

these tables, “Error” refers to the maximum norm pricing error, which is computed over all grid points of the approximation domain G . Other symbols have the same meanings as that in Table 2. Numerical results in Tables 3, 4, and 5 demonstrate again that the proposed ETI scheme outperforms the IMEX Euler based extrapolation scheme both in outer iteration numbers and CPU times, especially when the maturity time \bar{T} is large. Moreover, with the increasing of \bar{T} , the outer iteration numbers required by the ETI scheme do not increase while the ones by the extrapolation scheme increase, which is an another advantage of the ETI scheme over the extrapolation scheme.

Table 3: Numerical results for pricing the DBP option with maturity time $\bar{T} = 0.25$ by the ETI scheme and the extrapolation scheme respectively.

(m,n)	ETI		Extrapolation		Error	ratio
	out/inner	CPUtime	out/inner	CPUtime		
(10, 64)	9/6.00	0.07	55/7.45	0.37	4.26e-002	2.60
(20, 128)	18/8.00	0.37	55/9.22	0.87	1.64e-002	4.13
(40, 256)	18/9.50	1.13	55/9.85	2.25	3.96e-003	4.35
(80, 512)	18/10.67	4.52	55/10.51	7.68	9.11e-004	5.27
(160,1024)	18/11.11	18.86	55/10.73	30.81	1.73e-004	
(320,2048)	19/11.63	77.73	55/10.95	132.22		

Table 4: Numerical results for pricing the DBP option with maturity time $\bar{T} = 0.5$ by the ETI scheme and the extrapolation scheme respectively.

(m,n)	ETI		Extrapolation		Error	ratio
	out/inner	CPUtime	out/inner	CPUtime		
(10, 64)	15/6.93	0.13	66/8.18	0.51	2.12e-002	4.63
(20, 128)	18/8.89	0.42	66/10.02	1.13	4.58e-003	4.20
(40, 256)	16/10.00	1.10	66/10.55	3.31	1.09e-003	4.52
(80, 512)	16/10.88	4.30	66/10.94	10.42	2.41e-004	5.62
(160,1024)	16/11.50	17.64	66/11.27	39.43	4.29e-005	
(320,2048)	16/11.88	66.78	66/11.45	166.29		

5 Concluding remarks

In this paper, we consider approximating the product of a matrix exponential with block Toeplitz matrix and a vector, which arises from integrating a two dimensional PIDE in option pricing problems in the SVCJ model by the ETI scheme. The shift-invert Arnoldi

Table 5: Numerical results for pricing the DBP option with maturity time $\bar{T} = 1$ by the ETI scheme and the extrapolation scheme respectively.

(m,n)	ETI		Extrapolation		Error	ratio
	out/inner	CPUtime	out/inner	CPUtime		
(10, 64)	11/8.45	0.11	78/8.79	0.61	1.43e-002	14.57
(20, 128)	14/9.64	0.34	78/10.63	1.44	9.84e-004	3.84
(40, 256)	14/10.43	0.97	91/10.92	4.17	2.56e-004	3.84
(80, 512)	11/11.18	2.96	91/11.40	13.60	6.66e-005	4.46
(160,1024)	14/11.93	15.82	91/11.52	53.07	1.49e-005	
(320,2048)	14/12.14	59.84	91/11.71	229.14		

method is employed to fast compute this product, which results in an inner-outer iteration. To relieve the computational burden, the matrix splitting technique with multigrid method is proposed to deal with the shift-invert block Toeplitz matrix-vector product in each inner iteration. Numerical results are presented to demonstrate the efficiency of the proposed scheme. There still exact some problems that are needed to be considered further. The first one is to prove from the theoretical point of view that the semidiscrete matrix $A+B$ is a sectorial operator, which guarantees the fast convergence rate of the shift-invert Arnoldi method. The second one is to rigorously analyze the convergence of the splitting iteration scheme (3.3). These would be our future work.

Acknowledgements. The author is grateful to the anonymous reviewers for their comments and their effort in improving the paper.

References

- [1] L. ANDERSEN AND J. ANDREASEN, *Jump-diffusion processes: Volatility smile fitting and numerical methods for option pricing*, Rev. Derivatives Res., 4 (2000) pp. 231–262.
- [2] O. BARNDORFF-NIELSEN, *Process of normal inverse Gaussian type*, Finance Stoch., 2 (1998), pp. 41–68.
- [3] D. BATES, *Jumps and stochastic volatility: Exchange rate processes implicit in Deutsche Mark options*, Rev. Financial Stud., 9 (1996), pp. 69–107.
- [4] F. BLACK AND M. SCHOLES, *The pricing of options and corporate liabilities*, J. Polit. Econ., 81 (1973), pp. 637–654.
- [5] WILLIAM L. BRIGGS, VAN EMDEN HENSON, AND STEVE F. MCCORMICK, *A Multi-grid Tutorial*, 2nd ed., SIAM, Philadelphia, 2000.

- [6] P. CARR, H. GEMAN, D. MADAN, AND M. YOR, *The fine structure of asset returns: An empirical investigation*, J. Business, 75 (2002), pp. 305–332.
- [7] P. CARR AND L. WU, *Finite moment log stable process and option pricing*, J. Finance, 58 (2003), pp. 753–777.
- [8] R. CHAN AND X. JIN, *An Introduction to Iterative Toeplitz Solvers*, SIAM, Philadelphia, 2007.
- [9] Y. D’HALLUIN, P. FORSYTH AND K. VETZAL, *Robust numerical methods for contingent claims under jump diffusion*, IMA J. Numer. Anal., 25 (2005) pp. 87–112.
- [10] D. DUFFIE, J. PAN, AND K. SINGLETON, *Transform analysis and asset pricing for affine jump diffusions*, Econometrica, 68 (2000), pp. 1343–1376.
- [11] E. EBERLEIN, U. KELLER, AND K. PRAUSE, *New insights into smile, mispricing, and value at risk: the hyperbolic model*, J. Business, 71 (1998), pp. 371–405.
- [12] M. EIERMANN AND O. ERNST, *A restarted Krylov subspace method for the evaluation of matrix functions*, SIAM J. Numer. Anal., 44 (2006), pp. 2481–2504.
- [13] B. ERAKER, M. JOHANNES, AND N. POLSON, *The impact of jumps in volatility and returns*, J. Finance, 58 (2003), pp. 1269–1300.
- [14] L. FENG AND V. LINETSKY, *Pricing options in jump diffusion models: An extrapolation approach*, Oper. Res., 56 (2008), pp. 304–325.
- [15] S. HESTON, *A closed form solution for options with stochastic volatility with applications to bond and currency options*, Rev. Financial Stud., 6 (1993), pp. 327–343.
- [16] N. HIGHAM, *Functions of Matrices: Theory and Computation*, Society for Industrial and Applied Mathematics, Philadelphia, PA, USA, 2008.
- [17] M. HOCHBRUCK AND C. LUBICH, *On Krylov subspace approximations to the matrix exponential operator*, SIAM J. Numer. Anal., 34 (1997), pp. 1911–1925.
- [18] J. HULL AND A. WHITE, *The pricing of options on assets with stochastic volatilities*, J. Finance, 42 (1987), pp. 281–300.
- [19] S. KOU, *A jump diffusion model for option pricing*, Management Sci., 48 (2002), pp. 1086–1101.
- [20] S. LEE, X. LIU AND H. SUN, *Fast exponential time integration scheme for option pricing with jumps*, Numer. Linear Algebra Appl., 19 (2012), pp. 87–101.
- [21] S. LEE, H. PANG AND H. SUN, *Shift-invert Arnoldi approximation to the Toeplitz matrix exponential*, SIAM J. Sci. Comput., 32 (2010), pp. 774–792.

- [22] L. LOPEZ AND V. SIMONCINI, *Analysis of projection methods for rational function approximation to the matrix exponential*, SIAM J. Numer. Anal., 44 (2006). pp. 613–635.
- [23] D. MADAN, P. CARR, AND E. CHANG, *The variance gamma process and option pricing*, Eur. Finance Rev., 2 (1998), pp. 79–105.
- [24] R. MERTON, *Option pricing when underlying stock returns are discontinuous*, J. Financial Econom., 3 (1976), pp. 125–144.
- [25] I. MORET AND P. NOVATI, *RD-rational approximations of the matrix exponential*, BIT, 44 (2004), pp. 595–615.
- [26] H. PANG AND H. SUN, *Shift-invert Lanczos method for the symmetric positive semidefinite Toeplitz matrix exponential*, Numer. Linear Algebra Appl., 18 (2011), pp. 603–614.
- [27] M. POPOLIZIO AND V. SIMONCINI, *Acceleration techniques for approximating the matrix exponential operator*, SIAM J. Matrix Anal. Appl., 30 (2008), pp. 657–683.
- [28] N. RAMBEERICH, D. TANGMAN, A. GOPAUL, AND M. BHURUTH, *Exponential time integration for fast finite element solutions of some financial engineering problems*, J. Comput. Appl. Math., 224 (2009), pp. 668–678.
- [29] M. RUBINSTEIN, *Implied binomial trees*, J. Finance, 49 (1994), pp. 771–818.
- [30] Y. SAAD, *Analysis of some Krylov subspace approximations to the matrix exponential operator*, SIAM J. Numer. Anal., 29 (1992), pp. 209–228.
- [31] L. SHAMPINE, *Vectorized adaptive quadrature in Matlab*, J. Comput. Appl. Math., 211 (2008), pp. 131–140.
- [32] D. TANGMAN, A. GOPAUL, AND M. BHURUTH, *Exponential time integration and Chebychev discretisation schemes for fast pricing of options*, Appl. Numer. Math., 58 (2008), pp. 1309–1319.
- [33] J. VAN DEN ESHOF AND M. HOCHBRUCK, *Preconditioning Lanczos approximations to the matrix exponential*, SIAM J. Sci. Comput., 27 (2006), pp. 1438–1457.
- [34] Y. ZHANG, H. PANG, L. FENG, AND X. JIN, *Quadratic finite element and preconditioning for options pricing in the SVCJ model*, to appear in J. Comput. Finance.